AD-A095 755 STANFORD UNIV CALIF DEPT OF MATHEMATICS F/G 20/4
BUBBLE OR DROP DISTORTION IN A STRAINING FLOW IN TWO DIMENSIONS--ETC(U)
JAN 80 J VANDEN-BROECK, J B KELLER DAAG29-79-C-0222
UNCLASSIFIED ARO-16997.8-M NL

END
DATE FILMED
3 81
DTIC

UNCLASSIFIED

SECURITY CLASSIFICATION OF THIS PAGE (When Data Entered)

(2)

REPORT DOCUMENTATION PAGE

READ INSTRUCTIONS BEFORE COMPLETING FORM

1. REPORT NUMBER: 16997.8-M (19)	2. GOVT ACCESSION NO.: N/A AD-A095755 N/A
3. RECIPIENT'S CATALOG NUMBER	
4. TITLE (and Subtitle): Bubble or Drop Distortion in a Straining Flow in Two Dimensions (6)	5. TYPE OF REPORT & PERIOD COVERED: REPRINT
	6. PERFORMING ORG. REPORT NUMBER: N/A
7. AUTHOR(s): (10) Jean-Marc Vanden-Broeck, Joseph B. Keller (13)(6) (15)	8. CONTRACT OR GRANT NUMBER(s): DAAG29-79-C-0222
9. PERFORMING ORGANIZATION NAME AND ADDRESS: Stanford University, Stanford CA 94305 (11) 12 Jun 80	10. PROGRAM ELEMENT, PROJECT, TASK AREA & WORK UNIT NUMBERS: N/A
11. CONTROLLING OFFICE NAME AND ADDRESS: US Army Research Office, PO Box 12211, Research Triangle Park, NC 27709	12. REPORT DATE: Aug 80
	13. NUMBER OF PAGES: 5
14. MONITORING AGENCY NAME & ADDRESS (if different from Controlling Office)	15. SECURITY CLASS. (of this report): Unclassified
	15a. DECLASSIFICATION/DOWNGRADING SCHEDULE

16. DISTRIBUTION STATEMENT (of this Report)

Submitted for announcement only

DTIC ELECTE FEB 27 1981 S B

17. DISTRIBUTION STATEMENT (of the abstract entered in Block 20, if different from Report)

18. SUPPLEMENTARY NOTES

19. KEY WORDS (Continue on reverse side if necessary and identify by block number)

20. ABSTRACT (Continue on reverse side if necessary and identify by block number)

AD A095755

DTIC FILE COPY

DD FORM 1 JAN 73 1473 EDITION OF 1 NOV 65 IS OBSOLETE

UNCLASSIFIED 332577

SECURITY CLASSIFICATION OF THIS PAGE (When Data Entered)

Bubble or drop distortion in a straining flow in two dimensions

Jean-Marc Vanden-Broeck

Department of Mathematics, Stanford University, Stanford, California 94305

Joseph B. Keller

Departments of Mathematics and Mechanical Engineering, Stanford University, Stanford, California 94305

(Received 21 January 1980; accepted 16 May 1980)

The distortion of a two-dimensional bubble (or drop) in a straining flow of an inviscid imcompressible fluid is examined theoretically. Far from the bubble the stream function of the flow is assumed to be αxy, where α is a constant. Within the bubble the pressure is assumed to be a constant p_b, and the bubble surface is assumed to have a surface tension σ. Then, the shape of the bubble depends upon the single dimensionless constant $\gamma = 2(p_b - p_s)/(2\sigma\alpha)^{2/3}\rho^{1/3}$, where ρ is the fluid density, p_s is the stagnation pressure of the flow, and the size of the bubble is proportional to $(2\sigma/\rho\alpha^2)^{1/3}$. For γ large, it is found that the bubble tends to a circle of radius $(2\sigma/\rho\alpha^2)^{1/3}\,\gamma^{-1}$. As γ decreases, numerical solutions show that the bubble at first becomes a square with rounded corners. Then, it develops four horns or spikes with large curvature near their ends. Finally at $\gamma \sim -1.8$, the two sides of each spike touch each other near the tip and enclose a small bubble there. It is also found that there is a maximum value of the Weber number above which there is no steady solution.

I. INTRODUCTION AND FORMULATION

In the mixing of two fluids, a drop or bubble of one fluid will be distorted and possibly split into smaller parts because of the flow of the other fluid around it. In order to study this phenomenon, we consider the two-dimensional case of a drop or bubble of one fluid in a steady flow of another fluid, assumed to be inviscid and incompressible. We take into account the surface tension σ at the interface, but we ignore the flow inside the drop or bubble, assuming that the pressure is a constant p_b throughout it. From now on we shall write "bubble" to mean either bubble or drop.

In order to formulate this problem we assume that the stream function of the flow without the bubble is αxy, where α is a constant and x and y are Cartesian coordinates. This flow is symmetric about both the x and y axes, so we assume that the bubble and the flow around it will have the same symmetry. Then, it suffices to determine the flow only in the first quadrant $x \geq 0$, $y \geq 0$ (see Fig. 1).

We introduce dimensionless variables by choosing $(2\sigma/\rho\alpha^2)^{1/3}$ as the unit length and $(2\sigma\alpha/\rho)^{1/3}$ as the unit velocity. We also introduce the dimensionless potential function $b\varphi$ and stream function $b\psi$. Here, $b>0$ is a dimensionless constant to be chosen so that $\varphi = \frac{1}{2}$ and $\varphi = -\frac{1}{2}$ at the stagnation points on the x and y axes, respectively. We denote the streamline along the two axes and along the arc of the bubble boundary in the first quadrant by $\psi = 0$. In these variables $b\psi \sim xy$ and $b\varphi \sim (x^2 - y^2)/2$ at infinity, so that $b(\varphi + i\psi) \sim (x+iy)^2/2$ or, equivalently,

$$x + iy \sim (2b)^{1/2}(\varphi + i\psi)^{1/2} \tag{1}$$

at infinity. The flow occupies the region $\psi \geq 0$ of the φ, ψ plane, and the bubble boundary corresponds to the segment $-\frac{1}{2} < \varphi < \frac{1}{2}$ of the axis $\psi = 0$. The problem of finding the flow consists of determining $x + iy$ as an analytic function of $\varphi + i\psi$ in the half-plane $\psi \geq 0$ satisfying Eq. (1) at infinity. Then, the bubble surface is given by setting $\psi = 0$ in $x(\varphi + i\psi)$ and $y(\varphi + i\psi)$, and letting φ range from $-\frac{1}{2}$ to $\frac{1}{2}$. The symmetry conditions require that the bubble surface be normal to the x and y axes where it intersects them, which yields

$$y_\varphi(-\tfrac{1}{2}, 0) = x_\varphi(\tfrac{1}{2}, 0) = 0 \,. \tag{2}$$

On the bubble surface the pressure in the fluid, which is given by the Bernoulli equation, must differ from p_b by σk, where k is the curvature of the interface. This leads to the boundary condition

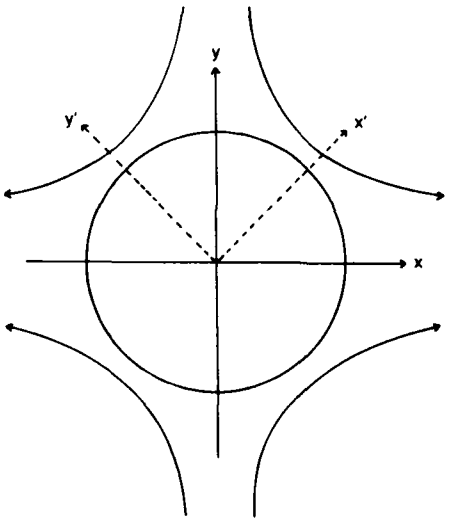

FIG. 1. The bubble, some stream lines of the flow, and the x and y axes are sketched. The x' and y' axes, used in Sec. V, are also indicated.

 0031-9171/80/081491-05$00.90

$$p_s - \rho q^2/2 = p_b - \sigma k, \quad \text{on} -\tfrac{1}{2} < \varphi < \tfrac{1}{2}, \quad \psi = 0. \tag{3}$$

Here, p_s, ρ, and q are, respectively, the stagnation pressure, density, and the speed of the fluid outside the bubble. In dimensionless variables (3) becomes

$$q^2 = k - \gamma, \quad \text{on} -\tfrac{1}{2} < \varphi < \tfrac{1}{2}, \quad \psi = 0\ , \tag{4}$$

where the dimensionless parameter γ is defined by

$$\gamma = 2(p_b - p_s)/(2\sigma\alpha)^{2/3}\rho^{1/3}\ . \tag{5}$$

The problem can be further simplified by requiring the bubble to be symmetric about the line $y = x$. This implies that

$$y_\varphi(-\varphi, 0) = -x_\varphi(\varphi, 0)\ , \quad -\tfrac{1}{2} < \varphi < \tfrac{1}{2}\ . \tag{6}$$

By using Eq. (6) we can restrict our analysis to the interval $0 < \varphi < \frac{1}{2}$.

II. REFORMULATION

It is convenient to reformulate the boundary value problem as an integro-differential equation by considering the function

$$(\varphi + i\psi)^{1/2}(x_\varphi + iy_\varphi) - (b/2)^{1/2},$$

which is analytic in the half-plane $\psi > 0$ and vanishes at infinity as a consequence of Eq. (1). Therefore, on $\psi = 0$, its real part is the Hilbert transform of its imaginary part. By symmetry its imaginary part vanishes on $\psi = 0$, $|\varphi| > \frac{1}{2}$ and therefore the Hilbert transform yields

$$\varphi^{1/2}x_\varphi(\varphi, 0) - \left(\frac{b}{2}\right)^{1/2} = \frac{1}{\pi}\int_0^{1/2} \frac{(\varphi')^{1/2}y_\varphi(\varphi', 0)}{\varphi' - \varphi}\, d\varphi' + \frac{1}{\pi}\int_{-1/2}^{0} \frac{(-\varphi')^{1/2}x_\varphi(\varphi', 0)}{\varphi' - \varphi}\, d\varphi'\ . \tag{7}$$

We now use the symmetry condition (6) to rewrite (7) in the form

$$x_\varphi(\varphi, 0) = \left(\frac{b}{2}\right)^{1/2}\varphi^{-1/2} + \frac{\varphi^{-1/2}}{\pi} \times \int_0^{1/2} (\varphi')^{1/2}y_\varphi(\varphi', 0)\left(\frac{1}{\varphi' - \varphi} + \frac{1}{\varphi' + \varphi}\right) d\varphi'\ . \tag{8}$$

Next, we express the boundary condition (4) in terms of x_φ and y_φ, noting that $q^2 = b^2(x_\varphi^2 + y_\varphi^2)^{-1}$. Then, (4) becomes

$$\frac{b^2}{x_\varphi^2 + y_\varphi^2} = \frac{y_\varphi x_{\varphi\varphi} - x_\varphi y_{\varphi\varphi}}{(x_\varphi^2 + y_\varphi^2)^{3/2}} - \gamma, \quad |\varphi| < \tfrac{1}{2}, \quad \psi = 0\ . \tag{9}$$

Now, (8) and (9) together constitute a nonlinear integro-differential equation for $y_\varphi(\varphi)$ in the interval $0 \le \varphi \le \frac{1}{2}$, $\psi = 0$. The symmetry conditions

$$x_\varphi(\tfrac{1}{2}, 0) = 0\ , \tag{10}$$

$$x_\varphi(0, 0) = -y_\varphi(0, 0)\ , \tag{11}$$

complete the formulation of the problem for $y_\varphi(\varphi, 0)$ and b. This formulation of the problem, and the numerical method to be described follows closely the work of Vanden-Broeck and Keller.[1,2]

III. NUMERICAL PROCEDURE

Before solving the problem we note that $y_\varphi(\varphi, 0)$ must be singular at $\varphi = \frac{1}{2}$ like $(\frac{1}{2} - \varphi)^{-1/2}$. Therefore, we eliminate this singularity by replacing φ with the new variable β defined by

$$\varphi = \tfrac{1}{2} - \beta^2\ . \tag{12}$$

Then, we introduce the N mesh points β_I given by

$$\beta_I = (I-1)/2^{1/2}(N-1), \quad I = 1, \ldots, N\ , \tag{13}$$

and the $N-1$ corresponding unknowns

$$y_I' = \left(\frac{\partial y}{\partial \beta}\right)_{\beta=\beta_I,\,\psi=0}, \quad I = 1, \ldots, N-1. \tag{14}$$

If we define y_N' by (14) with $I = N$, it then follows from (11) and (12) that

$$x_\beta(\beta_N, 0) = -y_N'\ . \tag{15}$$

Now, we define $\beta_{I+1/2} = (\beta_I + \beta_{I+1})/2$, and then consider $x_\beta(\beta_{I+1/2}, 0)$. We compute it from (8) rewritten in terms of β. However, the integrand contains the factor $(\varphi')^{1/2} = (\frac{1}{2} - \beta^2)^{1/2}$, which has a singular derivative at $\beta = 2^{-1/2}$. In order to integrate this factor accurately, we replace y_φ by $(y_\varphi - y_N') + y_N'$, use the trapezoidal rule with mesh point β_I on the intervals containing $y_\varphi - y_N'$, and analytically evaluate the integral containing y_N'. Then, $x_\beta(\beta_{I+1/2}, 0)$ is given in terms of the y_J'.

Next, we compute $y_\beta(\beta_{I+1/2}, 0)$, $x_{\beta\beta}(\beta_{I+1/2}, 0)$, and $y_{\beta\beta}(\beta_{I+1/2}, 0)$ in terms of the y_J' by using four-point difference formulae. From these expressions we calculate y_φ, $x_{\varphi\varphi}$ and $y_{\varphi\varphi}$ at $(\beta_{I+1/2}, 0)$, by noting that

$$y_\varphi = \frac{-y_\beta}{2\beta}$$

and

$$(x + iy)_{\varphi\varphi} = \frac{(x + iy)_{\beta\beta}}{4\beta^2} - \frac{(x + iy)_\beta}{4\beta^3}\ .$$

Then, we substitute these expressions into (9) at the $N-1$ points $(\beta_{I+1/2}, 0)$, $I = 1, \ldots, N-1$ to obtain $N-1$ nonlinear algebraic equations in the $N+1$ unknowns y_I', $I = 1, \ldots, N$ and b. The last two equations are obtained from (10) and (15) by using three-point Lagrange extrapolation formulae to evaluate their left sides.

The N nonlinear equations were solved by Newton's iteration method. For some large value of γ, the initial approximation for the bubble surface was taken to be a circular arc. Iterations were continued until the solution converged within a given tolerance. This solution was then used as the initial guess for a smaller value of γ and so on.

After a solution for the y_I' and b converged for some value of γ, the profile $x(\beta, 0)$, $y(\beta, 0)$ was obtained by integrating x_β and y_β. Typical profiles for various values of γ are shown in Fig. 2. For γ large the bubble surface is close to a circle of dimensionless radius γ^{-1}. For smaller values of γ, the bubble surface is close to a square with rounded corners. As γ decreases further the bubble surface elongates in the directions midway between the axes, developing four horns or spikes.

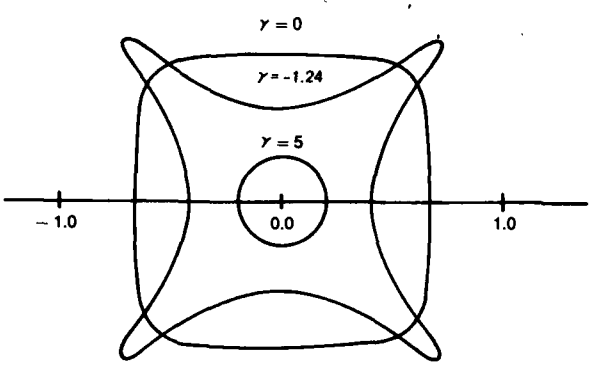

FIG. 2. Computed bubble profiles for various values of γ. These profiles were found by the method of Sec. III.

The efficiency of the numerical scheme was found to be limited by the high curvature at the ends of the spikes. Accurate solutions for $\gamma < -1.3$ could not be computed even with $N = 50$. Thus, in the last section we shall consider an analytical approach to determine the ultimate form of the horns as γ is further decreased.

From the numerical solution we can calculate the area A of the bubble and the potential energy V. The potential energy V is equal to the surface tension σ times the length of the surface. In dimensional variables we have

$$V = \left(\frac{2\sigma^4}{\rho\alpha^2}\right)^{1/3} 8 \int_0^{2^{-1/2}} [x_\beta^2(\beta,0) + y_\beta^2(\beta,0)]^{1/2}\, d\beta \,, \tag{16}$$

$$A = \left(\frac{2\sigma}{\rho\alpha^2}\right)^{2/3} 8 \left(- \int_0^{2^{-1/2}} y(\beta,0) x_\beta(\beta,0)\, d\beta + \tfrac{1}{2}[y(\beta,0)]_{\beta=2^{-1/2}}^2 \right) . \tag{17}$$

We also introduce the Weber number W defined by

$$W = A^{1/2}(\rho\alpha^2/2\sigma)^{1/3} . \tag{18}$$

The integrals in (16) and (17) were evaluated by the trapezoidal rule. The results are shown as functions of γ in Fig. 3.

We see that the potential energy V is a monotone decreasing function of γ. However, the dimensionless area A, which is equal to the square of the Weber number W^2, is not monotonic but has a maximum at $\gamma \sim -0.2$. Thus, the figure shows that there is a maximum or critical value of W^2 above which there is no steady solution of the kind considered here. This maximum value is $W^2 \sim 2.1$. The existence of a maximum Weber number has previously been found for a two-dimensional bubble or drop in a uniform potential flow by Vanden-Broeck and Keller,[2] and for a two dimensional drop in a Stokes' flow by Buckmaster and Flaherty[3] and by Vanden-Broeck.[4] In the three-dimensional case the corresponding results were obtained by Moore,[5] El Sawi,[6] and Miksis *et al.*[7] for potential flow and by Rallison and Acrivos[8] for Stokes' flow.

There are two solutions for each value of the Weber number in an interval below the maximum value. For the branch on the left of the maximum in Fig. 3, the potential energy V decreases as W increases, so this branch is probably unstable. For the branch on the right of the maximum, V increases as W increases, so it is probably stable.

IV. SOLUTION FOR γ LARGE

For γ large we seek the bubble surface as a small perturbation of a circle of radius γ^{-1}. Thus, we write it in polar coordinates r, θ as

$$r = \gamma^{-1} + \gamma^{-4}\rho(\theta) + O(\gamma^{-5}) \,. \tag{19}$$

The curvature k of this surface is given by

$$k = \gamma + \gamma^{-2}[\rho''(\theta) + \rho(\theta)] + O(\gamma^{-3}) \,. \tag{20}$$

Now, the unperturbed complex potential $\varphi_0 + i\psi_0$ is given as a function of $z = x + iy$ by

$$\varphi_0 + i\psi_0 = z^2/2 + 1/2\gamma^4 z^2 \,. \tag{21}$$

From (21) we see that on the circle of radius γ^{-1}, $\varphi_0 = \gamma^{-2} \cos 2\theta$ and, therefore, $q_0 = -2\gamma^{-1} \sin 2\theta$.

In the boundary condition (4) we use Eq. (20) for k and the preceding result for q_0. The terms in γ^{-2} lead to

$$\rho''(\theta) + \rho(\theta) = 4 \sin^2 2\theta \,. \tag{22}$$

The solution ρ of (22) satisfying $\rho'(0) = \rho'(\pi/4) = 0$, when used in (19), yields the result

$$r = \gamma^{-1} - 2(1 + \tfrac{1}{15}\cos 4\theta)\gamma^{-4} + O(\gamma^{-5}) \,. \tag{23}$$

We next substitute (23) into the definitions of V and A and get

$$V = (2\sigma^4/\rho\alpha^2)^{1/3}\, 2\pi(\gamma^{-1} - 2\gamma^{-4}) + O(\gamma^{-5}) \,, \tag{24}$$

$$A = (2\sigma/\rho\alpha^2)^{2/3}\, \pi(\gamma^{-2} - 4\gamma^{-5}) + O(\gamma^{-6}) \,. \tag{25}$$

The formulae (24) and (25) agree with the numerical results of Sec. III within 0.5% for $\gamma > 4$.

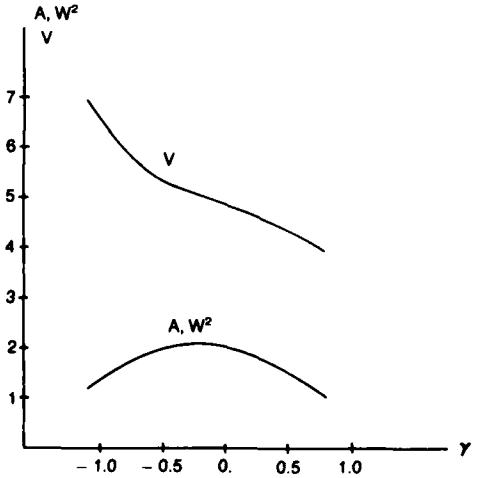

FIG. 3. Computed values of the bubble area A [in units of $(2\sigma/\rho\alpha^2)^{2/3}$] and potential energy V [in units of $(2\sigma^4/\rho\alpha^2)^{1/3}$] as functions of γ, based upon Eqs. (16) and (17). With this choice of units the lower curve is also a graph of W^2, the square of the Weber number.

V. THE LIMITING SHAPE OF THE BUBBLE

When γ is less than about -1.3, the bubble has four slender spikes. They are oriented along the lines $y = \pm x$, as shown in Fig. 2. Because the spikes are so slender, their shape can be found approximately by using the slender body theory for bubbles presented by Vanden-Broeck and Keller.[2] In lowest order, the flow about a symmetric slender bubble is approximated by the flow about a rigid plate lying along the center line of the bubble. In the present case the center lines of the four spikes consist of two straight line segments, each of some length $2a$, lying along the lines $y = \pm x$. We introduce the coordinates x', y' with axes along these lines, and find the potential $b\varphi(x', y')$ of the flow about these plates, requiring that at infinity $b\varphi \sim (x^2 - y^2)/2$. Evaluating this potential on the plate $y' = 0$, $x' > 0$ we obtain

$$b\varphi(x', 0) = (a^4 - x'^4)^{1/2}/2 \ . \tag{26}$$

By differentiating (26) we find that the flow speed q on the plate is

$$q(x', 0) = x'^3(a^4 - x'^4)^{-1/2}, \quad x' \geq 0 \ . \tag{27}$$

Before using q to get the bubble shape, we shall determine the half-length a of the center lines. We do so by requiring the suction force F, exerted by the flow on the end of a spike, to balance the surface tension 2σ. As we see in Ref. 9 [p. 412, Eq. (6.5.4)], $F = \pi\rho A^2/4$. Here, A is the coefficient in the expansion $b\varphi \sim Ar^{1/2} \times \cos\theta/2$ in terms of polar coordinates with their origin at the end of the plate. Upon setting $F = 2\sigma$ and introducing dimensionless variables we obtain

$$A^2 = 4/\pi \ . \tag{28}$$

From (26) we find that $A^2 = a^3$, so (28) yields

$$a = (4/\pi)^{1/3} \ . \tag{29}$$

We next use (27) for q in (4) and approximate the curvature k by $-\eta_{x'x'}(x')$. Here, the equation of the bubble is $y' = \eta(x')$ for x', y' in the first quadrant of the x, y plane, i.e., for $x' \geq y' \geq 0$. Then Eq. (4) becomes

$$\eta_{x'x'} = -x'^6(a^4 - x'^4)^{-1} - \gamma \ . \tag{30}$$

At the end of the spike we require

$$\eta(a) = 0. \tag{31}$$

In addition, by symmetry, the bubble must be normal to the y axis where it crosses that axis. In the primed coordinates this axis is the line $x' = y'$, and this symmetry condition becomes

$$\eta_{x'} = -1 \ , \tag{32}$$

where $x' = \eta(x')$.

Upon integrating Eq. (30) twice and using Eq. (31), we obtain

$$\begin{aligned}\eta(x') = {} & \frac{x'^4}{12} - \gamma\frac{x'^2}{2} - \frac{a^3}{4}(a - x')\log(a - x') \\ & - \frac{a^3}{4}(a + x')\log(a + x') - \frac{a^4}{4}\log(a^2 + x'^2) \\ & + \frac{a^3 x'}{2}\tan^{-1}\frac{x'}{a} - \beta(x' - a) - \frac{a^4}{12} + \gamma\frac{a^2}{2} \\ & + \frac{a^4}{2}\log 2a + \frac{a^4}{4}\log 2a^2 - \frac{a^4\pi}{8} \ .\end{aligned} \tag{33}$$

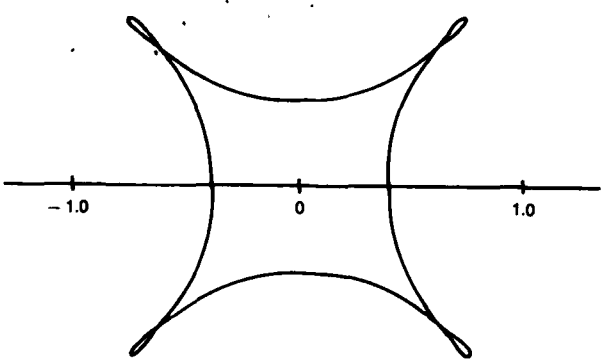

FIG. 4. The ultimate form of the bubble at $\gamma = -1.8$, when opposite sides of each spike just touch one another and enclose a small sub-bubble near the tip.

The integration constant β in (33) is to be found in order to make $\eta(x')$ satisfy (32). For each value of γ, (32) can be solved numerically for β by iteration. Then, (33) gives the approximate shape of the bubble.

By solving for β in this way for various values of γ, and examining (33), we find that opposite sides of each spike touch each other at $\gamma \approx -1.8$. Then, each spike contains a small sub-bubble near its tip, as shown in Fig. 4. This profile represents the ultimate form of our family of solutions. For smaller values of γ opposite sides of each spike cross one another, which is physically inadmissible. We could obtain physically acceptable solutions for $\gamma < -1.8$ by allowing the pressure in the sub-bubble to be different from that in the main bubble. We shall not find them because they are probably unstable. It is likely that the sub-bubble would become detached from the main bubble if γ were decreased below -1.8.

Finally, we shall indicate how the preceding slender body theory can be improved upon when it is used to find a bubble with a sub-bubble at the tip of each spike. We first replace each sub-bubble by a straight segment of length l. Then, we calculate the flow around the main bubble terminated by these segments, and the shape of the main bubble, using the numerical method of Sec. III. This yields a two-parameter family of solutions, with parameters γ and l. Then, for each γ we find the $l(\gamma)$ for which the forces balance at the tip of each segment. Next, we solve the equation analogous to (30) for the function $\eta(x')$ which gives the surface of the sub-bubble, requiring the surface position and slope to be continuous where the main bubble meets the sub-bubble. At last, we determine the pressure in the sub-bubble by requiring that $\eta = 0$ at the end of the sub-bubble. If this pressure is required to be the same as that in the main bubble, we find the value of γ corresponding to the ultimate configuration shown in Fig. 4.

ACKNOWLEDGMENTS

We want to thank Professor Andreas Acrivos for having suggested this problem.

This work was supported by the Office of Naval Re-

search, the National Science Foudation, the Air Force Office of Scientific Research, and the Army Research Office.

[1]J.-M. Vanden-Broeck and J. B. Keller, J. Fluid Mech. **98**, 161 (1980).
[2]J.-M. Vanden-Broeck and J. B. Keller, J. Fluid Mech. (to be published).
[3]J. D. Buckmaster and J. E. Flaherty, J. Fluid Mech. **60**, 625 (1973).
[4]J.-M. Vanden-Broeck, Phys. Fluids (to be published).
[5]D. W. Moore, J. Fluid Mech. **23**, 749 (1965).
[6]M. El Sawi, J. Fluid Mech. **62**, 163 (1974).
[7]M. Miksis, J.-M. Vanden-Broeck, and J. B. Keller, J. Fluid Mech. (to be published).
[8]J. M. Rallison and A. Acrivos, J. Fluid Mech. **89**, 191 (1978).
[9]G. K. Batchelor, *Introduction to Fluid Dynamics* (Cambridge University Press, Cambridge, 1967).

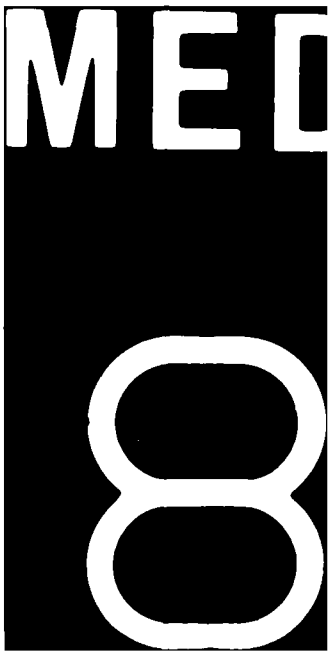
MED
8